

# Electromagnetic follow-ups in the era of forecasting gamma-ray bursts

Subtitle here if needed

Sarp Akcay<sup>1,2</sup>, Antonio Martin-Carrillo<sup>3</sup>, and Morgan Fraser<sup>3</sup>

<sup>1</sup> Theoretisch-Physikalisches Institut, Friedrich-Schiller-Universität Jena, 07743, Jena, Germany

<sup>2</sup> School of Mathematics & Statistics, University College Dublin, Belfield, Dublin 4, Ireland

<sup>3</sup> School of Physics, University College Dublin, Belfield, Dublin 4, Ireland

December 12, 2018

## ABSTRACT

The discovery of gravitational waves from merging compact objects has opened up a new window on the Universe. Planned third generation gravitational wave detectors such as the Einstein Telescope will potentially deliver hundreds of such events at redshifts below  $z \sim 0.1$ . Finding electromagnetic counterparts to these events will be a major observational challenge. We demonstrate how the Einstein Telescope will provide advance warning of such events on a timescale of hours, based on the low frequency emission from the pre-merger system. In addition, we suggest how this early warning enables prompt identification of any electromagnetic counterpart.

**Key words.** gravitational waves – gamma-ray bursts – kilonovae

## 1. Introduction

With the first direct detection of gravitational waves (GWs) in 2015 by the Advanced Laser Interferometer Gravitational-Wave Observatory (Advanced LIGO; Abbott et al. 2016), gravitational wave astronomy moved from prospect to reality. The first GW source observed by Advanced LIGO, GW150914, matched the signal predicted for the merger of two black holes with masses 36 and 29  $M_{\odot}$ .

Only two years after GW15014, the Advanced LIGO and Virgo gravitational wave observatories detected GW170817, with a waveform consistent with the merger of two neutron stars (Abbott et al. 2017c). A spatially and temporally coincident short Gamma Ray Burst (GRB) was also seen by the *Fermi* and *INTEGRAL* satellites (Abbott et al. 2017b). This discovery sparked a global effort to find the counterpart of GW170817 at optical wavelengths, which resulted in the identification of AT2017gfo less than 11 hours later (Abbott et al. 2017d). AT2017gfo faded exceptionally rapidly, and displayed cool temperatures and lines from unusual r-process elements at exceptionally high velocities (Smartt et al. 2017; Arcavi et al. 2017; Pian et al. 2017; Coulter et al. 2017; Kilpatrick et al. 2017). These characteristics marked AT2017gfo as a kilonova; a transient powered by the radioactive decay of short-lived nuclides formed in the merger of two neutron stars.

The detection of electromagnetic (EM) counterparts to GWs from merging neutron stars is of exceptional significance for astrophysics. Kilonovae are the predominant site for r-process nucleosynthesis, and so play a critical role in the chemical evolution of galaxies. If a kilonova can be identified and associated with a host galaxy of known redshift, then the degeneracy between inclination angle and distance inherent to a GW signal can be broken. This in turn allows the opening angle of the GRB

jet to be constrained, something that has been done for a handful of GRBs to date (Jin et al. 2018). GW sources can also be used to independently determine the Hubble constant  $H_0$  (Abbott et al. 2017a).

The identification of AT2017gfo as the counterpart to GW170817 was realised by the ability of Advanced LIGO-Virgo to localise the GW signal to  $\sim 30$  deg<sup>2</sup>. In addition, at only 40 Mpc, GW170817 was exceptionally close. This enabled the EM counterpart to be identified through targeted observations of galaxies at this distance within the GW localisation region (Coulter et al. 2017). Unfortunately, such a strategy is only feasible for the nearest GW sources, and rapidly becomes unrealisable beyond  $\sim 100 - 200$  Mpc, both as the number of galaxies within the search volume increases, and as the fraction of galaxies with reliable redshifts decreases. This embarrassment of riches is a serious obstacle for identifying EM counterparts to GW transients that will be detected by Einstein Telescope in the 2030s (Abernathy et al. 2011).

Einstein Telescope (ET) will consist of three V-shaped interferometers which eliminate blind spots and further allow it to construct a null stream (Sathyaprakash et al. 2012) which can be used to veto spurious events (Wen & Schutz 2005). Additionally, ET will be a xylophone (Hild et al. 2010), i.e., a multi-band detector capable of delivering high sensitivities both at low frequencies ( $\sim 5$  Hz) and high frequencies ( $\sim 100$  Hz). Here, we focus on the C configuration (ET-C) which offers the highest low-frequency sensitivity as shown in Fig. 1. ET-C will detect  $\gtrsim O(10^3)$  binary neutron star inspirals per year out to 1 Gpc (Akcay 2018). A subset of these sources will be close enough that they will be detected a few hours before their respective mergers (Akcay 2018), hence opening up the possibility of alerting EM observatories to conduct follow-up observations *before, during* and after the prompt gamma-ray bursts.

To fully exploit the prospect of multi-messenger astronomy, a number of wide-field survey telescopes are either operational, in commissioning, or under construction. Foremost among these is the Large Synoptic Survey Telescope (LSST; LSST Science Collaboration et al. 2009), which has an 8.4 m primary mirror, and will image  $9.6 \text{ deg}^2$  in a single pointing. Construction of LSST is well underway with full survey operations starting in 2023. Apart from LSST, the majority of current and next-generation survey telescopes have a relatively small mirror, but a large camera, and are designed to observe  $\sim 10 - 50 \text{ deg}^2$  in a single pointing to a limiting magnitude of  $\sim 20 - 22$ . ZTF (Bellm 2014), GOTO (Dyer et al. 2018) and ATLAS (Tonry 2011) are all currently operational at present, while BlackGEM is currently under construction (Bloemen et al. 2016).

There has been a considerable amount of discussion in the literature as to the optimal strategy to identify an EM counterpart to future GW transients (Gehrels et al. 2016; Coward et al. 2011; Ghosh et al. 2016; Chan et al. 2017; Siellez et al. 2014; Antolini & Heyl 2016). In most cases however, a large number of candidates will be found within the search region, for which further spectroscopic follow-up observations will be required. This spectroscopic classification bottleneck will remain a problem into the foreseeable future.

Our aim here is to demonstrate exciting EM follow-up studies that can be done by taking advantage of the early GW warning capability of ET. The ability of ET to detect inspiraling compact objects  $\sim$  hrs before the merger has been described in detail by Akcay (2018), and in this Letter we present a brief summary of these results and their implications for follow-up observations of electromagnetic counterparts.

This letter is organized as follows: Sect. 2 provides more details on ET, Sect. 3 investigates the implications of optical follow-up. We use  $f$  to denote the quadrupole GW frequency in the detector frame.  $G$  is Newton's constant and  $c$  is the speed of light.

## 2. Einstein Telescope

In this section, we compute advance warning times ( $T_{\text{AW}}$ ) ET will provide. The computational details are provided in Akcay (2018). Consider a binary neutron star (BNS) system with component masses  $m_1, m_2$  inspiraling at a luminosity distance  $D$  with a corresponding redshift  $z$ . For GW frequencies of interest here ( $f \lesssim 10 \text{ Hz}$ ), the binary undergoes an adiabatic inspiral dominated by the emission of leading-order (quadrupole) gravitational radiation. By balancing the power emission in GWs to the rate of change of binding energy, we obtain the frequency evolution of the GW frequency

$$\dot{f} = \frac{96}{5} \pi^{8/3} \frac{(G\mathcal{M}_c)^{5/3}}{c^5} f^{11/3}, \quad (1)$$

where  $\mathcal{M}_c = (1+z)(m_1 m_2)^{3/5} (m_1 + m_2)^{-1/5}$  is the redshifted chirp mass. After fixing an integration constant, Eq. (1) can be integrated to yield the time left to merger at a given frequency, usually called the inspiral time

$$\begin{aligned} \tau_{\text{insp}}(f) &= \frac{5}{256\pi} \frac{c^5}{(\pi G \mathcal{M}_c)^{5/3}} f^{-8/3} \\ &= 16.72 \text{ minutes} \left( \frac{1.219 M_\odot}{\mathcal{M}_c} \right)^{5/3} \left( \frac{10 \text{ Hz}}{f} \right)^{8/3}. \end{aligned} \quad (2)$$

This result can be supplemented with a post-Newtonian series up to  $\mathcal{O}(c^{-7})$  (Blanchet 2014), but the resulting expressions only change  $\tau_{\text{insp}}$  by  $\lesssim 2\%$ .

To obtain  $T_{\text{AW}}$  we must choose a value of  $f$ . A passing GW induces a response in a given interferometer (IFO) known as the GW strain. In frequency domain, the norm of the GW strain is given by  $|\tilde{h}(f)| = A h_0 f^{-7/6} |Q|$ , where  $A = \pi^{-2/3} (5/24)^{1/2}$ ,  $h_0 = c(1+z)^{-1} \tilde{M}^{5/6} / D$  with  $\tilde{M} = G\mathcal{M}_c c^{-3}$  and  $Q$  is the IFO quality factor which is a function of source sky location and inclination angles  $\{\theta, \phi, \iota\}$ , and the relative detector-source polarization angle  $\psi$ .

The IFO response to a GW strain is quantified in terms of a signal-to-noise ratio (SNR). As we can not a priori know the angles  $\{\theta, \phi, \iota, \psi\}$ , we use an angle-RMS-averaged SNR, appropriate for a detector with triangular topology like ET

$$\rho_{\text{ET}}(f_1, f_2) = \frac{6}{5} A h_0 (1+z)^{-1/6} \left[ \int_{f_1}^{f_2} df' \frac{f'^{-7/3}}{S_n(f')} \right]^{1/2}, \quad (3)$$

where  $\sqrt{S_n(f)}$  is the *amplitude spectral density* of the detector (also called detector noise) and the factor of  $6/5$  in Eq. (3) is due to RMS-averaging (Akcay 2018). For a given source,  $\rho_{\text{ET}}$  may vary by  $\sim \pm 30\%$  compared to the average (3), but will always be  $> 0$  because of ET's all-sky coverage.

We define  $T_{\text{AW}}$  to be the time left to merger from the moment of detection defined as follows: let  $f_0$  be the frequency at which the GW strain equals the detector noise, i.e.,  $\sqrt{S_n(f_0)} = 2\sqrt{f_0} \tilde{H}_{\text{ET}}(f_0)$  where  $\tilde{H}_{\text{ET}}(f) = 3h_0 f^{-7/6} / 5$ ; the instant of detection is given by  $\tilde{f} > f_0$  such that  $\rho_{\text{ET}}(f_0, \tilde{f}) = 15$ . Thus  $T_{\text{AW}} = \tau_{\text{insp}}(\tilde{f})$ . The total accumulated SNR is given by  $\rho_{\text{tot}} = \rho_{\text{ET}}(f_0, f_{\text{ISCO}})$ , where  $f_{\text{ISCO}}$  is the frequency at which the inspiral transitions to plunge. Here, we use the standard approximation from general relativity:  $f_{\text{ISCO}} \approx c^3 [6^{3/2} \pi G(m_1 + m_2)(1+z)]^{-1} \approx 1571(1-z) \left( \frac{2.8 M_\odot}{m_1 + m_2} \right) \text{ Hz}$  for  $z \ll 1$ . We chose a conservative threshold SNR of 15.

$D$  now fully determines  $T_{\text{AW}}$ . In Fig. 1 we display the GW strain for four canonical ( $m_1 = m_2 = 1.4 M_\odot$ ) BNS inspirals at  $D = 100, 200, 400, 600 \text{ Mpc}$ . ET-C's noise is the thick, red curve with the best sensitivity for  $f \lesssim 10 \text{ Hz}$ . Note that, as is standard, the inspiral GW strains scale as  $\sqrt{f} f^{-7/6} = f^{-2/3}$  (Colpi & Sesana 2017), hence are straight lines with slope  $= -2/3$ . The frequencies  $f_0$  where these straight lines intersect ET-C's noise curve are distinguishable below 2 Hz. We list the advance warning times along with the total SNRs for these sources in Table 1, where we show that ET-C is capable of providing up to five hours of early warning before merger.

**Table 1.** Forecasting capabilities of the C configuration of Einstein Telescope.  $D$  is the luminosity distance and  $z$  the corresponding redshift computed assuming a flat  $\Lambda$ CDM universe with  $\Omega_\Lambda = 0.6911$ ,  $\Omega_m = 0.3089$ ,  $H_0 = 67.74 \text{ km s}^{-1} \text{ Mpc}^{-1}$  (Adam et al. 2016).  $\tilde{f}$  is the threshold frequency at which ET-C accumulates SNR of 15.  $T_{\text{AW}} \equiv \tau_{\text{insp}}(\tilde{f})$  [see Eq. (2)].  $\rho_{\text{tot}}$  is the total SNR for each inspiral. Last column lists the event rates within concentric shells of radius  $D$  and thickness  $100 \text{ Mpc}$ .

$D \text{ (Mpc)}$	$z$	$\tilde{f} \text{ (Hz)}$	$T_{\text{AW}} \text{ (hrs)}$	$\rho_{\text{tot}}$	$R_{\text{av}}^{\text{max}} \text{ (yr}^{-1}\text{)}$
100	0.022	3.3	5.3	365	$1.54^{+3.20}_{-1.22}$
200	0.044	4.1	2.9	182	$10.8^{+22.4}_{-8.54}$
300	0.065	4.66	1.9	121	$29.3^{+60.8}_{-23.2}$
400	0.085	5.1	1.5	90.5	$57.0^{+118}_{-45.1}$
500	0.10	5.4	1.2	72	$93.9^{+195}_{-74.4}$
600	0.12	5.7	1.03	60	$140^{+291}_{-111}$

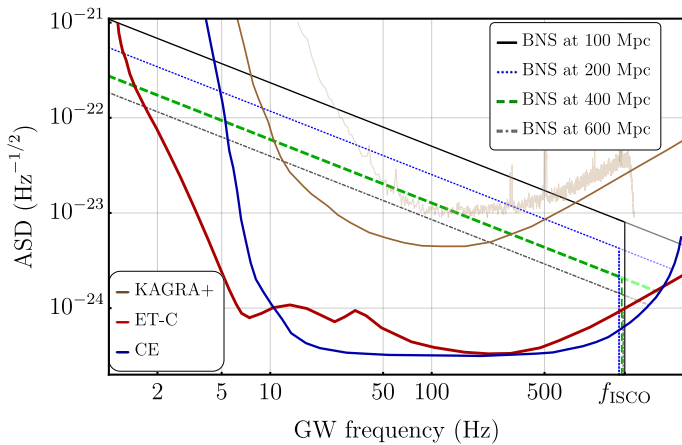


**Fig. 1.**  $1.4M_{\odot} - 1.4M_{\odot}$  inspiralling BNS systems sweeping across the sensitivity band of Einstein Telescope’s C configuration (thick red curve). The solid (black), dotted (blue), dashed (green), and dot-dashed lines (gray) lines are the redshift-corrected angle-RMS-averaged GW strains,  $2\sqrt{f}\dot{H}_{\text{ET}}$ , at luminosity distances of  $D = 100, 200, 400, 600$  Mpc, respectively. The vertical lines with correspondingly identical patterns (colors) mark the redshifted ISCO frequencies  $(1+z)^{-1}f_{\text{ISCO}}$  at which point we terminate each inspiral. As the true ISCO frequency is likely larger than  $f_{\text{ISCO}}$  (Marronetti et al. 2004), the inspirals would continue to nearly 2 kHz indicated by the faded lines in the plot. We also show the strain sensitivity of Cosmic Explorer (thick blue) and KAGRA+ (brown curve). The faint brown curve represents the sensitivity of Advanced LIGO during GW170817.

### 2.1. Event rates for binary neutron star inspirals

We base our event rate calculations on  $R = 1540^{+3200}_{-1220} \text{ Gpc}^{-3} \text{ yr}^{-1}$  inferred from GW170817 (Abbott et al. 2017c) consistent with  $110 - 3840 \text{ Gpc}^{-3} \text{ yr}^{-1}$  (LIGO-Virgo Collaboration 2018). This translates roughly to  $R(D \leq 600 \text{ Mpc}) = 330^{+690}_{-260} \text{ yr}^{-1}$ . We partition this volume into concentric shells each 100 Mpc thick. For each shell, we show the event rates in Table 1.

We see from Table 1 that within  $z \lesssim 0.1$ , ET-C will annually detect GWs from  $\sim 40$  to 600 BNS transients. Roughly 7% of these will be within 200 Mpc yielding  $T_{\text{AW}} \gtrsim 3$  hours which means that EM observatories will be alerted  $\sim 3 - 40$  times yearly with the prospect of observing births of kilonovae. If we assume that future EM observatories could respond with  $T_{\text{AW}} = 1$  hour warning, then all BNS transients within 600 Mpc become possible candidates for merger-kilonovae observations. In this case, early warnings would be sent by ET at least once a week and at most three times per day.

### 2.2. Source localisation estimations

ET will have poor source localisation because all three of its IFOs will be at the same location. However, as our findings in Table 1 indicate, ET-C will detect BNS inspirals hours before the merger during which time the Earth will have rotated by  $\sim 10^\circ - 50^\circ$ . Therefore, within 1 Gpc, ET alone will localise  $\sim 20\%$  of the sources to within  $100 \text{ deg}^2$ ,  $2\%$  to within  $20 \text{ deg}^2$ , and  $0.5\%$  to within  $10 \text{ deg}^2$  (Zhao & Wen 2018)<sup>1</sup>. Rescaling to  $D = 400 \text{ Mpc}$ , corresponding to  $T_{\text{AW}} = 1.5 \text{ hrs}$ , we obtain  $\gtrsim 5$  yearly BNS transients with  $\Delta\Omega \lesssim 10 \text{ deg}^2$  and  $\gtrsim 20$  transients with  $\Delta\Omega \lesssim 20 \text{ deg}^2$ .

<sup>1</sup> Zhao & Wen (2018) perform their calculations for ET-D which in fact has slightly worse sensitivity for  $f \lesssim 5 \text{ Hz}$  than ET-C, cf. Fig. 19 of Pitkin et al. (2011)

Our above approximations on localisation should be taken as the pessimistic case as ET will be not be operating alone. Currently suggested companion detectors are the Japanese cryogenic detector KAGRA (Akutsu et al. 2017, 2018), LIGO’s successor Voyager (Berger et al. 2016), its “relative” in India (Unnikrishnan 2013), and finally, Cosmic Explorer (CE): the third generation US detector with 40 km armlength (Abbott et al. 2017). Assuming a three-detector network consisting of ET and two CEs with a total network SNR  $> 12$  and two detectors each with SNR  $> 5$ , Mills et al. (2018) find that half of signals will be localised to within  $1 \text{ deg}^2$  out to a redshift of  $z \sim 0.25$ . However, this survey is not concerned with issuing sufficiently early warnings to EM facilities. The problem is that only ET has the extreme low-frequency sensitivity enabling  $T_{\text{AW}} \sim \text{hours}$ . The other detectors will not accumulate any SNR from BNS inspirals in the  $f \lesssim 5 \text{ Hz}$  domain<sup>2</sup>. However, CE will be sensitive enough to accumulate SNR from 5 Hz for BNSs with  $D \lesssim 400 \text{ Mpc}$  (Fig. 1). Given that its sensitivity increases steeply between 5 and 10 Hz, CE will accumulate SNR = 5 with 1.5 hours left to merger and SNR = 15 with 1.25 hours left resulting in a total network SNR,  $\rho_{\text{net}} \equiv (\rho_{\text{ET}}^2 + \rho_{\text{CE}}^2)^{1/2} = \{18.8, 27.4\}$  for  $\tau_{\text{insp}} = \{1.5, 1.25\}$  hours, respectively. As localisation improves with increasing SNR, this means that an initial  $\Delta\Omega$  of  $\sim 100 \text{ deg}^2$  can be reduced as the BNS inspirals through its second to last hour before the merger.

This region can be further decreased once the BNS enters a third detector’s bandwidth, which will most likely be the mid-2020s-upgraded KAGRA+ with its strain sensitivity shown as the brown curve in Fig. 1. Using the same analysis as for CE, we find that KAGRA+ will pick up a 400-Mpc inspiral at  $\sim 10 \text{ Hz}$  and will accumulate SNR = 5 within a minute. For a 100-Mpc source, KAGRA+ would accumulate SNR  $> 15$  more than a half hour before the merger. Thus, for nearby sources, even KAGRA+ sensitivity could contribute to pre-merger localisation efforts. Given that LSST requires  $\sim 5$  minutes to point anywhere in the sky, KAGRA’s contribution will matter. Once again, this is a rather pessimistic estimation as we expect the 2030s KAGRA to be more sensitive than the brown curve of Fig. 1.

In short, within 400 Mpc, we can annually expect five BNS transients to be localised to  $10 \text{ deg}^2$  1.5 hours before the merger. We can expect an additional  $\sim 15$  more with initial localisation of  $\sim 20 \text{ deg}^2$  which we expect will be narrowed down to  $\sim 10 \text{ deg}^2$  about one hour before the merger. We envision a three-stage localisation procedure whereby ET conducts the operations alone until  $f \sim 5 \text{ Hz}$  — roughly two hours before merger — at which point CE joins in and, finally, around  $f \sim 10 \text{ Hz}$  KAGRA+ starts accumulating SNR with  $\gtrsim 15$  minutes left to merger.

## 3. Implications for optical follow-up of GW detections

Identifying an optical or near-infrared (NIR) counterpart to a GW is an observational challenge. If a GW is only localised to tens, or even hundreds of square degrees, then we must survey a large area of the sky to find an EM counterpart. While large format CCDs make taking imaging of an area of  $\sim 100 \text{ deg}^2$  relatively straightforward, we must identify our EM counterpart of interest among the many unrelated astrophysical transients that we expect by chance within the same area. Thus far, this has relied upon large scale efforts to spectroscopically classify credible candidates that are found within the sky localisation of a

<sup>2</sup> There is a prospect for improving LIGO’s low-frequency end called LIGO-LF (Yu et al. 2018).

GW. For example, for the BH merger GW151226, Smartt et al. (2016) found 49 candidate transients within  $290 \text{ deg}^2$ , and obtained spectra for 20 of these. Such a survey strategy is clearly an inefficient use of scarce telescope time.

The early warning obtained for future GW events discussed in Sect. 2 offers an alternative approach for finding EM counterparts. In brief, if we can detect a GW with  $\sim 1 \text{ hr}$  advance warning, and can localise it to  $\sim 50 \text{ deg}^2$  or better, then we can obtain imaging of this area both immediately prior to, and after, the merger happens. Since the merger will be the only thing that has changed over such a short period of time, identifying an EM counterpart in difference imaging becomes straightforward.

While this section focuses on the optical/NIR part of the EM spectrum, we also considered the implications of an early GW warning at higher energies. Gamma-ray instruments have large field of views of the order of  $1 - 2 \text{ sr}$  resulting on a high probability of detecting the prompt emission of the merger by chance. Currently proposed missions, like THESEUS (Amati et al. 2018), will have a field of view limited almost exclusively by Earth and thus, an early warning system would not have any significant impact. The detection of the X-ray prompt emission (below  $5 \text{ keV}$ ) could have significant scientific value, however most of the instruments sensitive at those energies have fields of view of the order of  $\text{arcmin}^2$ . Currently, the JEM-X instrument onboard INTEGRAL is the only one instrument with a large enough field of view ( $25 \text{ deg}^2$ ). From the missions currently under study, only THESEUS would have an X-ray instrument with a large field of view ( $1 \text{ sr}$  in the  $0.3\text{--}5 \text{ keV}$ ). However, its sensitivity ( $10^{-10} \text{ erg cm}^{-2} \text{ s}^{-1}$  in  $1000 \text{ s}$ ) will not be enough to detect the prompt emission of most NS-NS or NS-BH mergers.

### 3.1. The rates and nature of contaminants

There are broadly three classes of contaminants that we must consider when searching for EM counterparts to GWs; stellar variables and flares such as cataclysmic variables (CV); variability in Active Galactic Nuclei (AGN); and supernovae (SNe). The first class of contaminants show a strong dependence on Galactic latitude (Drake et al. 2014), and are concentrated in the disk of the Milky Way. In addition, for at least some CVs a quiescent counterpart will be visible in deep images, or in other cases prior outbursts may have been detected. We hence expect that CVs and other variable stars will be a relatively minor source of contamination for EM counterpart searches. This is further borne out by Smartt et al. (2016), who found only 3 of 49 potential counterparts to GW151226 to be stellar.

AGN can often be identified through their historical lightcurves, which may show previous variability, or through the presence of a cataloged x-ray or radio counterpart. Given the relatively straightforward removal of stellar and AGN contaminants, we are left with SNe as the dominant contaminant. Again, in the case of GW151226 88% of potential counterparts turned out to be SNe. Within a magnitude limited survey around three quarters of events detected will be Type Ia SNe (Li et al. 2011), due to their luminosity. So, to first order, our main source of contamination when searching for EM counterparts of GW events will be Type Ia SNe.

We ran Monte Carlo simulations to obtain an estimate of the number of unrelated transients that may be found in a search for an EM counterpart to a GW transient. We took the volumetric Type Ia SN rate from Dilday et al. (2010), and assumed that the GW event could be localised to a region of  $\sim 30 \text{ deg}^2$ . We further assumed an optical survey with a cadence of 4 days and a limiting magnitude  $m_r \sim 22$ , and that the kilonova had an absolute

magnitude of  $M_r = -15$  at peak. We then calculated the number of Type Ia SNe that would be detected by the survey with a magnitude comparable ( $\pm 1 \text{ mag}$ ) to the kilonova, and where the SN would have not been detected on the previous image taken of the field four nights earlier. The results of this are shown in Fig. 2, where we find that for a GW source at a distance of a few hundred Mpc, we will typically have four unrelated SNe Ia that are impossible to distinguish from a kilonova solely on the basis of single filter imaging. In the worst case scenarios, we may have as many as ten contaminants that are observationally similar to the kilonova.

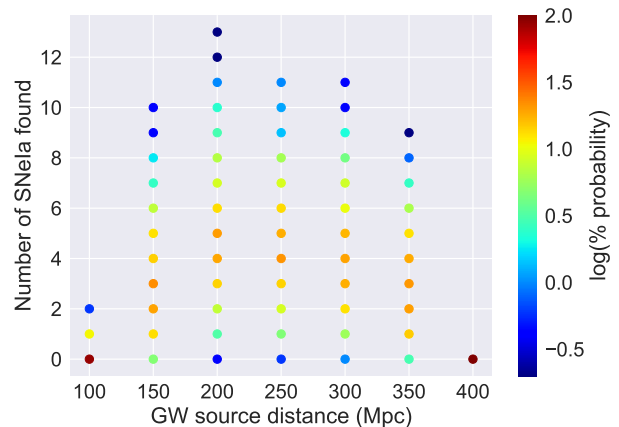


**Fig. 2.** The probability of finding a given number of SNe Ia (that are likely to be confused with a kilonova), as a function of distance. We assume a survey with a four night cadence reaching  $m_r \lesssim 22$ , a GW source localised to  $30 \text{ deg}^2$ , and a kilonova  $M_r = -15$ .

This calculation should be taken as an approximate guide, and the exact numbers of contaminants will vary with a number of factors. Higher-cadence transient surveys, and better localisation of GW events will reduce the number of contaminants found. On the other hand, simply increasing the depth of a survey will not necessarily improve matters; while some SNe will be detected earlier (and hence ruled out) when their lightcurves are still rising, greater numbers of more distant SNe will also be detected. In any case though, it is reasonable to expect that even in the most favourable scenarios we will always have more than a single plausible candidate counterpart to any future GWs.

### 3.2. A proposed strategy for EM counterpart detection

We have demonstrated that unrelated SNe Ia will be found within the region to which a GW is localised, and that a few of these are going to appear as new sources with comparable magnitude to a potential kilonova. There are two main reasons why this is a problem. Obtaining a spectrum of a kilonova and  $\sim 5$  unrelated SNe Ia will take commensurately longer.

The second reason why unrelated transients within the GW localisation region is a problem, is that it makes it much harder to obtain spectra of potentially rapidly fading BH-NS mergers, or of the very early ( $< 1 \text{ hr}$ ) evolution. If we have five sources of comparable magnitude, and it takes  $\sim 1 \text{ hr}$  to obtain a spectrum of each, we will only obtain a spectrum of the correct candidate in  $< 1 \text{ hr}$  in a minority of cases. The early warning from ET offers a solution to both of these problems. We propose that as soon as sufficient SNR is accumulated to localise a GW to  $\sim 20 \text{ deg}^2$  or

better, we take a set of images for that region of the sky *before* the merger occurs.

The LSST can reach a  $5\sigma$  limiting magnitude of  $r \sim 24.3$  with  $2 \times 15$  s images. The readout times for each exposure will be 2 s, and as the field of view of LSST is  $9.6 \text{ deg}^2$ , we will likely be able to cover the entire GW footprint in a small number of pointings. Even allowing 5 minutes for slewing of the telescope, it is likely that obtaining pre-merger images will take at most 10 minutes. Once the merger occurs, then we would take a second set of images. These would be subtracted from the pre-merger template images taken  $< 1$  hr before; and the kilonova should be the only thing that has changed over this brief period, making it trivial to identify.

**SA: Brief summary here. We showed that ..**

*Acknowledgements.* S. A. acknowledges support by the EU H2020 under ERC Starting Grant, no. BinGraSp-714626. MF is supported by a Royal Society - Science Foundation Ireland University Research Fellowship.

## References

- Abbott, B. P., Abbott, R., Abbott, T. D., et al. 2016, *Physical Review Letters*, 116, 061102
- Abbott, B. P., Abbott, R., Abbott, T. D., et al. 2017a, *Nature*, 551, 85
- Abbott, B. P., Abbott, R., Abbott, T. D., et al. 2017b, *ApJ*, 848, L13
- Abbott, B. P., Abbott, R., Abbott, T. D., et al. 2017c, *Physical Review Letters*, 119, 161101
- Abbott, B. P., Abbott, R., Abbott, T. D., et al. 2017d, *ApJ*, 848, L12
- Abbott, B. P. et al. 2017, *Class. Quant. Grav.*, 34, 044001
- Abernathy, M., Acernese, F., Ajith, P., et al. 2011, *Einstein gravitational wave Telescope Conceptual Design Study*, Tech. rep., European Commission
- Adam, R. et al. 2016, *Astron. Astrophys.*, 594, A1
- Akcay, S. 2018, *Annals der Physik*, 441, 1186
- Akutsu, T., Cadonati, L., Cavaglià, M., et al. 2017, in *15th International Conference on Topics in Astroparticle and Underground Physics (TAUP 2017)* Sudbury, Ontario, Canada, July 24–28, 2017
- Akutsu, T. et al. 2018, *PTEP*, 2018, 013F01
- Amati, L., O’Brien, P., Götz, D., et al. 2018, *Advances in Space Research*, 62, 191
- Antolini, E. & Heyl, J. S. 2016, *MNRAS*, 462, 1085
- Arcavi, I., Hosseinzadeh, G., Howell, D. A., et al. 2017, *Nature*, 551, 64
- Bellm, E. 2014, in *The Third Hot-wiring the Transient Universe Workshop*, ed. P. R. Wozniak, M. J. Graham, A. A. Mahabal, & R. Seaman, 27–33
- Berger, B. et al. 2016, *What Comes Next for LIGO? 2016 LIGO-DAWN Workshop II*, <https://wiki.ligo.org/pub/LSC/LIGOWorkshop2016/WebHome/Dawn-II-Report-SecondDraft-v2.pdf>
- Blanchet, L. 2014, *Living Rev. Rel.*, 17, 2
- Bloemen, S., Groot, P., Woudt, P., et al. 2016, in *Proc. SPIE, Vol. 9906, Ground-based and Airborne Telescopes VI*, 990664
- Chan, M. L., Hu, Y.-M., Messenger, C., Hendry, M., & Heng, I. S. 2017, *ApJ*, 834, 84
- Colpi, M. & Sesana, A. 2017, in *An Overview of Gravitational Waves: Theory, Sources and Detection*, ed. G. Auger & E. Plagnol, 43–140
- Coulter, D. A., Foley, R. J., Kilpatrick, C. D., et al. 2017, *Science*, 358, 1556
- Coward, D. M., Gendre, B., Sutton, P. J., et al. 2011, *MNRAS*, 415, L26
- Dilday, B., Smith, M., Bassett, B., et al. 2010, *ApJ*, 713, 1026
- Drake, A. J., Gänsicke, B. T., Djorgovski, S. G., et al. 2014, *MNRAS*, 441, 1186
- Dyer, M. J., Dhillon, V. S., Littlefair, S., et al. 2018, in *Society of Photo-Optical Instrumentation Engineers (SPIE) Conference Series, Vol. 10704, Society of Photo-Optical Instrumentation Engineers (SPIE) Conference Series*, 107040C
- Gehrels, N., Cannizzo, J. K., Kanner, J., et al. 2016, *ApJ*, 820, 136
- Ghosh, S., Bloemen, S., Nelemans, G., Groot, P. J., & Price, L. R. 2016, *A&A*, 592, A82
- Hild, S., Chelkowski, S., Freise, A., et al. 2010, *Class. Quant. Grav.*, 27, 015003
- Jin, Z.-P., Li, X., Wang, H., et al. 2018, *ApJ*, 857, 128
- Kilpatrick, C. D., Foley, R. J., Kasen, D., et al. 2017, *Science*, 358, 1583
- Li, W., Leaman, J., Chornock, R., et al. 2011, *MNRAS*, 412, 1441
- LIGO-Virgo Collaboration. 2018 [arXiv:1811.12907]
- LSST Science Collaboration, Abell, P. A., Allison, J., et al. 2009, *ArXiv e-prints* [arXiv:0912.0201]
- Marronetti, P., Duez, M. D., Shapiro, S. L., & Baumgarte, T. W. 2004, *Phys. Rev. Lett.*, 92, 141101
- Mills, C., Tiwari, V., & Fairhurst, S. 2018, *Phys. Rev.*, D97, 104064
- Pian, E., D’Avanzo, P., Benetti, S., et al. 2017, *Nature*, 551, 67
- Pitkin, M., Reid, S., Rowan, S., & Hough, J. 2011, 14
- Sathyaprakash, B. et al. 2012, *Class. Quant. Grav.*, 29, 124013, [Erratum: *Class. Quant. Grav.* 30, 079501 (2013)]
- Sielles, K., Boër, M., & Gendre, B. 2014, *MNRAS*, 437, 649
- Smartt, S. J., Chambers, K. C., Smith, K. W., et al. 2016, *ApJ*, 827, L40
- Smartt, S. J., Chen, T.-W., Jerkstrand, A., et al. 2017, *Nature*, 551, 75
- Tonry, J. L. 2011, *PASP*, 123, 58
- Unnikrishnan, C. S. 2013, *Int. J. Mod. Phys.*, D22, 1341010
- Wen, L. & Schutz, B. F. 2005, *Class. Quant. Grav.*, 22, S1321
- Yu, H. et al. 2018, *Phys. Rev. Lett.*, 120, 141102
- Zhao, W. & Wen, L. 2018, *Phys. Rev.*, D97, 064031